

An Improved Technique for Measurement of Gas Diffusion Anisotropy in Lung

K. Emami¹, S. Kadlecak¹, S. Pickup¹, J. M. Woodburn¹, J. Zhu², J. Yu¹, V. Vahdat¹, M. Ishii³, R. Cadman¹, S. Rajaei¹, T. Nakayama¹, C. Cox¹, R. Guyer¹, M. Law¹, M. Stephen⁴, J. Shrager², D. A. Lipson⁵, W. Gefter¹, and R. Rizi¹

¹Department of Radiology, University of Pennsylvania, Philadelphia, PA, United States, ²Department of Surgery, University of Pennsylvania, Philadelphia, PA, United States, ³Department of Otolaryngology, Johns Hopkins University, Baltimore, MD, United States, ⁴Pulmonary, Allergy, and Critical Care Division, University of Pennsylvania Medical Center, Philadelphia, PA, United States, ⁵Department of Pulmonology, University of Pennsylvania, Philadelphia, PA, United States

Introduction: The apparent diffusion coefficient (ADC) of hyperpolarized Helium is believed to be a useful diagnostic probe of pulmonary airway structure. Preliminary studies suggest that changes in the Helium ADC in lung tissue are correlated with the changes in structure induced by pulmonary diseases, especially in emphysema patients [1]. Furthermore, the ADC is capable of detecting changes in lung structure long before currently available diagnostic methods. The lung structure is known to be anisotropic and it is therefore believed that observation of the full diffusion tensor will reveal aspects of lung microstructure that are not evident in diffusion tensor trace measurements. In the present work the methodology for observation of the full Helium diffusion tensor is developed and demonstrated on phantoms and normal rat lungs.

Methods: A phantom consisting of a 50.5 mm circular loop of plastic tubing (ID=1.1mm, OD=2.05mm) was constructed (Figure 1.a). The gas entry and exit ports formed a discontinuity in the circumference of the loop as indicated in the figure. The phantom was used to study anisotropic diffusion in a system with *a priori* knowledge of the diffusion process. ADC measurements were performed along the three primary Cartesian coordinates. Four different combinations of bipolar gradients (Figure 1.b) were utilized: *Shaped* (with fixed ramp time) and *unshaped* (with fixed slew rate) gradients are shown in Figure 1.c. It is known that the contribution of background gradients to the observed diffusion decay can be eliminated by application of pairs of diffusion gradients of opposite sign. This can be achieved either by application of two sets of diffusion gradients within the same data acquisition (*single acquisition*) or by performing two studies with a single pair of gradients having inverted amplitude and taking the image product of the results (*double acquisition*). ADC measurements were performed for a wide range of diffusion times ($\Delta=0.5\text{ms}\sim3\text{ms}$). In order to verify the measurements of ADC anisotropy in the loop, A Monte Carlo simulation of diffusion in a loop was developed for comparison with the experimental observations. The simulation was performed by tracking a large number of individual particles undergoing Brownian motion and their accumulated phase during the diffusion-sensitizing gradients. The mean time between direction-changing collisions was set to reproduce the experimentally determined diffusion coefficient for ${}^3\text{He}$ in ${}^3\text{He}$, and boundary conditions were such that the particles reflected specularly at the tube inner surface. ADC anisotropy measurements were also performed *in vivo* in a group of healthy rats. Images were acquired using the modified diffusion-weighted gradient echo pulse sequence, during two separate back-to-back breath-holds (six images each time) corresponding to b -values = 0, 6.77, 4.50, 2.76, 1.32, and $0\text{s}/\text{cm}^2$, with $\Delta=1.5\text{ms}$. Other imaging parameters include: FOV=6cm, thickness=10mm, matrix=64x64 and flip angle=5°. The trace of the diffusion tensor was also measured in the animal studies.

Results and Conclusion: Of the possible four combinations of diffusion gradients, the *Double Acquisition Shaped* pulse protocol was the most robust and sensitive to diffusion anisotropy in the loop phantom studies. Figure 2.a shows the three-component ADC measurements in the loop phantom, with $\Delta=0.5\text{ms}\sim3\text{ms}$. The diffusion time dependency of the measurements is observed as a vertical shift in the curves (smaller Δ values yield larger ADC values). Experimental results show a good resemblance to that of Monte Carlo simulation (Figure 2.b). It should be noted that although the simulated and experimental results become indistinguishable in the case of restricted diffusion, the experimentally determined ADC values never reach the theoretical free diffusion coefficient ($\sim2.05\text{cm}^2/\text{sec}$) in the least restricted regions of the phantom. This is likely due to restriction of the gas by the phantom. Figure 3 shows three-component ADC measurements in a healthy rat lung, along with trace diffusion tensor and diffusion anisotropy images. The majority of the voxels in the lung exhibit isotropic diffusion. Certain regions however, including the major bronchi branching points and edges of the lobes exhibit diffusional anisotropy. Directional angles of the ADC vector can reveal other aspects of diffusion anisotropy. Shown on the last row of Figure 3, are maps of angles formed by each pair of the three ADC components (RO-PE, PE-SL and SL-RO respectively). Regional variation of these orientations (specially noticeable near apex and base) were very similar among the studied rats.

Conclusions: An optimized pulse sequence for measurement of gas diffusion anisotropy is presented and experimental results were consistent with Monte Carlo simulations of the diffusion process. The technique was successfully implemented on rats and diffusional anisotropy maps of lung tissue were obtained in these animals. The diffusional anisotropy maps were highly reproducible in normal rat lung.

Acknowledgements: This work was supported by NIH grants R01-HL64741, R01-HL077241, and P41-RR02305.

References: [1] DA Yablonskiy, *et al.* Quantitative *in vivo* assessment of lung microstructure at the alveolar level with hyperpolarized ${}^3\text{He}$ diffusion MRI. *Proc Natl Acad Sci U S A*. 2002 March 5; 99(5): 3111–3116.

[2] TE Conturo, *et al.* Encoding of anisotropic diffusion with tetrahedral gradients: a general mathematical diffusion formalism and experimental results. *Magn Reson Med* 1996; 35:399–412.

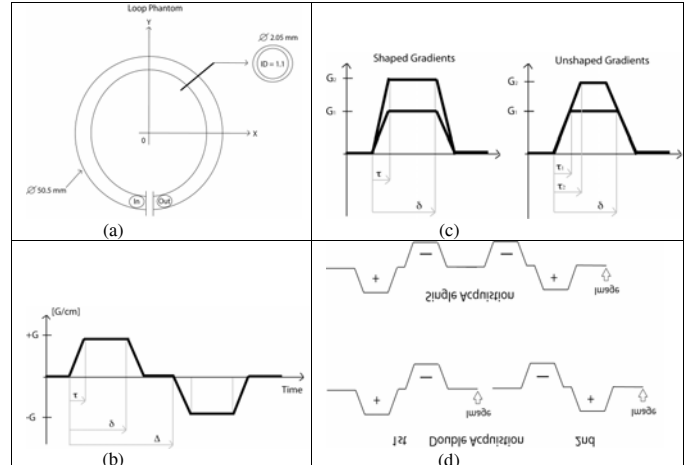


Figure 1. (a) Loop phantom; (b) Diffusion-sensitizing bipolar gradient; (c) Shaped and unshaped gradients; (d) Double- and single-acquisition ADC imaging sequences.

Images were acquired using the modified diffusion-weighted gradient echo pulse sequence, during two separate back-to-back breath-holds (six images each time) corresponding to b -values = 0, 6.77, 4.50, 2.76, 1.32, and $0\text{s}/\text{cm}^2$, with $\Delta=1.5\text{ms}$. Other imaging parameters include: FOV=6cm, thickness=10mm, matrix=64x64 and flip angle=5°. The trace of the diffusion tensor was also measured in the animal studies.

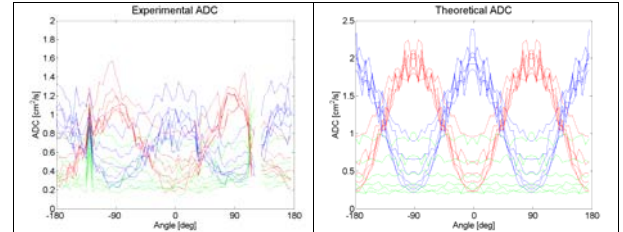


Figure 2. (a) Experimental measurement of the three primary components of ADC in the loop phantom (red:x, blue:y, green:z) for various diffusion times ranging from 500μs to 3ms (the discontinuity around $\theta = 120^\circ$ is where the tubes leave the imaging slice as gas entry/exit ports); (b) The corresponding theoretical ADC values obtained from a Monte-Carlo simulation in the loop phantom.

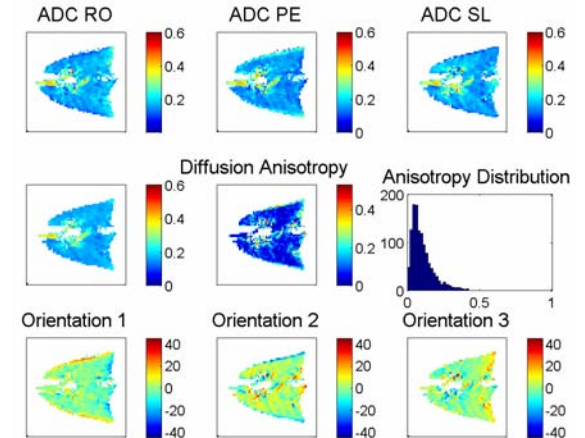


Figure 3. (Top) ADC maps in three primary directions; (Middle) Directionally averaged diffusion and anisotropy maps; (Bottom) Spatial distribution of ADC vector orientation angles.